

Discovery of Phthalazinone Derivatives as Novel Hepatitis B Virus Capsid Inhibitors

Wuhong Chen,[#] Feifei Liu,[#] Qiliang Zhao,[#] Xinna Ma, Dong Lu, Heng Li, Yanping Zeng, Xiankun Tong, Limin Zeng, Jia Liu, Li Yang,^{*} Jianping Zuo,^{*} and Youhong Hu^{*}

Cite This: <https://dx.doi.org/10.1021/acs.jmedchem.0c00346>

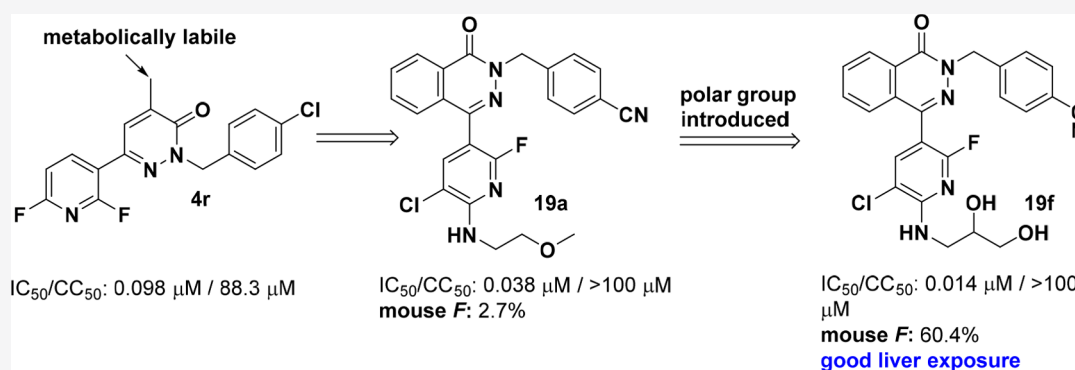
Read Online

ACCESS |

Metrics & More

Article Recommendations

Supporting Information



ABSTRACT: HBV capsid assembly has been viewed as an attractive target for new antiviral therapies against HBV. On the basis of a lead compound **4r**, we further investigated this target to identify novel active compounds with appropriate anti-HBV potencies and improved pharmacokinetic (PK) properties. Structure–activity relationship studies based on metabolic pathways of **4r** led to the identification of a phthalazinone derivative **19f** with appropriate anti-HBV potencies (IC₅₀ = 0.014 ± 0.004 μM *in vitro*), which demonstrated high oral bioavailability and liver exposure. In the AAV-HBV/mouse model, administration of **19f** resulted in a 2.67 log reduction of the HBV DNA viral load during a 4-week treatment with 150 mg/kg dosing twice daily.

INTRODUCTION

Hepatitis B virus (HBV) infection is a global public health issue with an estimated 250 million people chronically infected worldwide.¹ Among those, one-quarter of the patients are likely to develop serious liver diseases such as cirrhosis and hepatocellular carcinoma.² The current therapies for HBV infection are limited to nucleos(t)ide analogues (lamivudine, tenofovir, or entecavir (ETV), etc.) and interferons (IFNs).^{3,4} These two types of therapies can effectively suppress HBV replication, successfully delay liver disease progression, greatly reduce liver cancer incidence, and significantly improve long-term survival. However, both present major challenges: nucleos(t)ide therapies typically require lifetime treatment to prevent viral rebound, while IFNs-based therapies are associated with poor tolerance, limited responsiveness, and frequent adverse effects.⁵ Current HBV treatments do not offer a satisfactory clinical cure rate for chronic HBV infection.⁶

HBV capsid assembly is an essential step in the HBV life cycle, which can be interrupted to block HBV core protein aggregation and efficiently inhibit the synthesis of HBV DNA production.⁷ Therefore, it is considered an attractive target for new antiviral therapies against HBV. During the past decade, several chemotypes of capsid assembly modulators (or effectors) were reported (Figure 1).^{8,9} The heteroaryl-

dihydropyrimidine (HAP) compounds represented by compound **1** (Bay 41-4109),¹⁰ prevented the normal assembly of core proteins leading to aberrant capsid formation. **2** (GLS-4) and **3** (HAP-R10) are new generations of HAP analogues featuring 6-morpholine substituents and 2-thioazolyl groups attached to the core scaffold.^{11–15} By contrast, the phenylpropenamide (PPA) derivative **4** and the sulfamoylbenzamide (SBA) **5** act as HBV pgRNA encapsidation blockers, which accelerate the assembly of normal empty capsids.^{16–21}

The capsid assembly modulators were found to be able to disrupt capsid formation and subsequently inhibit HBV pgRNA encapsidation, reverse transcription, and DNA synthesis.^{22,23} Previously, we found a novel class of pyridazinone derivative **6** (**4r**) through HBV DNA-free capsid formation that showed potent antiviral activity (IC₅₀ = 0.087 ± 0.002 μM) with low cytotoxicity (CC₅₀ = 90.6 ± 2.06 μM),

Received: February 26, 2020

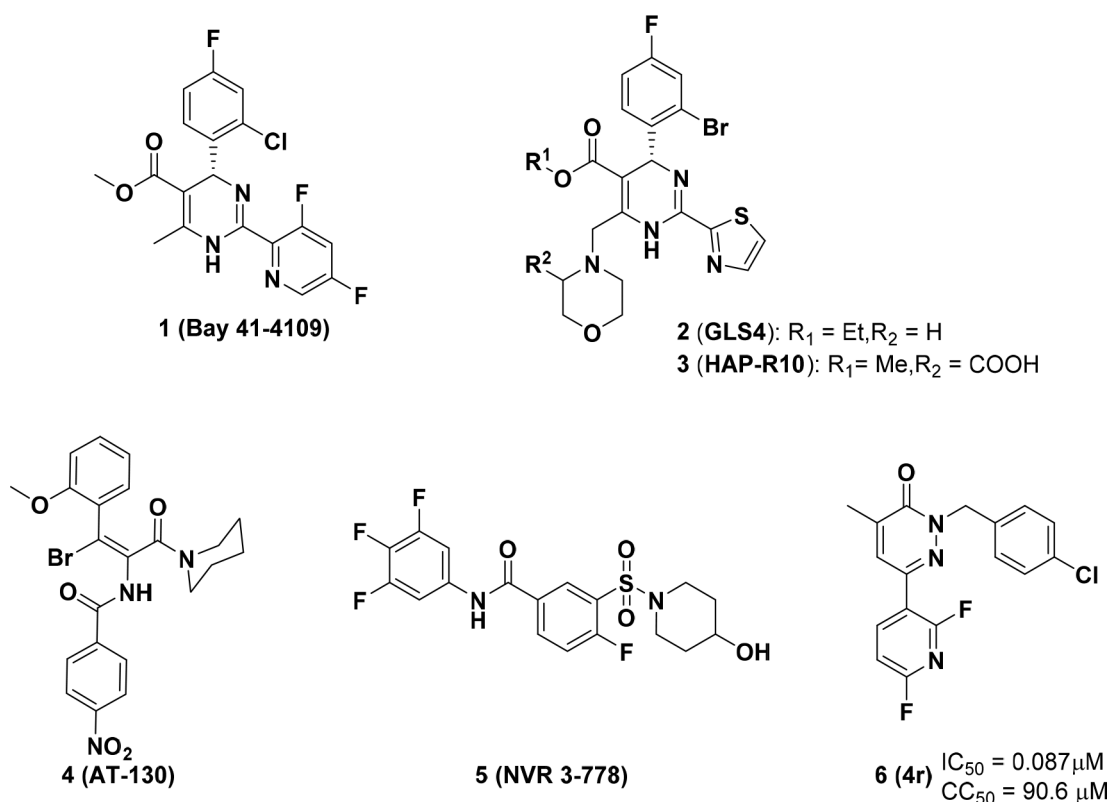


Figure 1. Chemical structures of representative HBV capsid assembly modulators.

Table 1. Single-Dose Pharmacokinetics of 4r in SD Rats^a

dose (mg/kg)	T _{1/2} (h)	T _{max} (h)	C _{max} (ng/mL)	AUC _{0-t} (h·ng/mL)	Cl _{obs} (mL min ⁻¹ kg ⁻¹)	V _{ss_obs} (mL/kg)	F (%)
po (20)	2.96 ± 0.15	0.25	352 ± 147	1095 ± 372			25.3 ± 8.59
iv (2)	2.03 ± 0.782			428 ± 47.6	77.6 ± 8.18	5.81 ± 2.53	

^aSingle-dose pharmacokinetics (SDPK) studies of 4r were carried out in SD rats according to standard procedures. The major parameters, including half-life (T_{1/2}), T_{max}, maximal concentration (C_{max}), the area under the curve (AUC_{0-t}), plasma clearance (Cl_{obs}), volume of distribution at steady state (V_{ss_obs}), and oral bioavailability (F), were reported.

sensitivity to nucleoside analogue-resistant HBV mutants, and synergistic effects with nucleoside analogues in HepG2.2.15 cells.²⁴ These results confirmed 4r as an attractive lead compound for further investigation in the treatment of HBV infection. Although the rat single dose pharmacokinetics (SDPK) profile (Table 1) of 4r showed moderate plasma clearance (Cl) (77.6 mL min⁻¹ kg⁻¹) and acceptable oral bioavailability (F) (25%), the exposure of compound 4r in liver could not be detected (see Supporting Information, Figure S1). We also tested the single-dose pharmacokinetics (Table S1) and liver distribution of 4r (Figure S1) in mice, which showed the low oral bioavailability and no exposure of 4r in liver. The metabolic stability of 4r in liver microsomes of humans, monkeys, dogs, rats, and mice was examined to identify any significant difference in the metabolic rate of 4r. After incubation for 60 min with human, monkey, dog, rat, and mouse liver microsomes, 34%, 73%, 79%, 64%, and more than 95% of the prototype drugs were metabolized from the relative UV area of 4r, respectively (Table 2). Most of compound 4r in mice was metabolized after the incubation with mouse liver microsomes for 60 min. Although compound 4r was more stable in human liver microsomes than in mouse, *in vivo* drug efficacy has to be evaluated in HDI mouse models. From the analysis of the metabolites for 4r (Table 2), the major

metabolite is oxide M1 (Figure 2). Comparing with the metabolic pathway of its analogue S4a²⁴ (with *p*-F phenyl substitution at 6-position of pyridazinone) in human liver microsomes with GSH (Table S2 and Figure S2), we hypothesized that the methyl substituent on the pyridazinone moiety could be easily oxidized. In this paper, we focus on the replacement of pyridazinone moiety to find the new phthalazinone scaffold and further SAR study to afford this novel anti-HBV lead compound with the improved PK profiles.

RESULTS AND DISCUSSION

Design and Structure–Activity Relationship (SAR).

First, 4-methylpyridazinone moiety replacements were designed, synthesized, and evaluated in HepG 2.2.15 cells (Table 3). The hydroxymethylated product 10a maintained anti-HBV activity with an IC₅₀ of 0.17 μM. However, the carboxylic acid 10b, which might be easily oxidized from 10a *in vivo*, lost the activity completely. The ester 10c and methoxyl substitution 10d at 4-position of pyridazinone also lost antiviral activity. The substitutions with cyclopropyl or isopropyl (10e and 10f), which could be beneficial for the prevention of the oxidation *in vivo*, decreased the activity dramatically. 4,5-Disubstituted pyridazinone derivatives 10g and 10h also reduced the potency. When the replacements of pyridazinone with pyrazinone,

Table 2. Information of Metabolites of 4r in Liver Microsomes of Human, Monkey, Dog, Rat and Mouse

metabolite name	m/z	formula	error (ppm)	t _R (min)	LC-MS area (×10 ³)					UV area (240 nm)						
					inactive microsomes	human	monkey	dog	rat	mouse	inactive microsomes	human	monkey	dog	rat	mouse
M0 parent	348.0722	C ₁₇ H ₁₂ N ₃ O ₂ F ₂ Cl	3.5	7.3	27.6	13.5	5.42	3.09	7.40	1.00	125	82.0	34.1	26.3	44.8	<5
M1 parent + O	364.0672	C ₁₇ H ₁₂ N ₃ O ₃ F ₂ Cl	3.7	6.4		2.64	8.30	5.97	3.05	10.3		51.3	113	84.6	56.7	117
M2 parent + O + O	380.0616	C ₁₇ H ₁₂ N ₃ O ₄ F ₂ Cl	2.1	5.5						0.79						15.4

pyridinone, phthalazinone gave **10i**, **10k**, **10j**, and **10l**, only compound **10l** with a phthalazinone scaffold retained the comparable anti-HBV activity with an IC₅₀ of 0.30 μM. On the basis of our previous SAR study (Table S3), 4-chlorobenzyl attached to the N atom of pyridazinone core can be changed by 4-cyanobenzyl group to keep the equitable activity. Compound **10m** was synthesized and showed moderate anti-HBV activity with low cytotoxicity compared to **4r**.

Next, the distribution of **10m** by oral administration was evaluated in ICR (CD-1) mice. **10m** showed high exposure in the liver at 1, 3, 8 h and dismissed after 24 h by po 20 mg/kg administration (see Supporting Information, Figure S3). The preferential liver distribution of **10m** could be beneficial to treat chronic HBV infections, which was targeted at the tissue.

Our previous research indicated that the fluorine atom at the 2-position of pyridine ring could form two hydrogen bonds with the Trp102 and Ser106 residues of capsid protein, which may contribute to the improved antiviral activity.²⁴ Further optimization and SAR exploration based on phthalazinone scaffold were carried out to keep F substitution at the 2-position of the pyridine moiety in Table 4.

Introducing substitution at the 6-position of pyridine **18a**, **18b**, and **18d–18f** maintained activity except compound **18c**, which contained an amide group and is different from the SAR of pyridazinone derivatives.²⁴ We speculated that the replacement of the core structure might change the electronic density and binding space slightly. Extending the group at the 6-position of pyridine (compound **18g**) yielded comparable inhibitory activity. Due to synthetic feasibility, 5-chloro substituted compound **19a** was obtained and significantly exhibited anti-HBV activity with low toxicity. The observed high activity may be a result of pyridine electronic density changes or increasing the hydrogen bond of Cl atom with the protein. Since the diverse side chain at the 6-position of pyridine could adjust the physical property of the compound, we modified this area with an unchanged 5-chloro substitution. With a terminated *N,N*-dimethyl (**19b**) and carbonyl group (ester **19c** and acid **19d**), the compounds showed the moderate anti-HBV activities. With a hydroxyl group at the terminal end of the side chain, compound **19e** also exhibited reliable antiviral activity with acceptable toxicity. On the basis of **19e**'s activity, we extended the side chain's hydroxy group to improve solubility (**19f**). **19f** showed excellent anti-HBV activity with an IC₅₀ value of 0.014 μM and CC₅₀ > 100 μM. These findings indicated that this diverse side chain could be tolerated with extended chemical space for further investigation. Since compound **19f** was a racemic mixture, the two enantiomers were synthesized. It was found that the *R*-configuration analogue **19h** showed better anti-HBV activity than the *S*-isomer **19g** with low toxicity. The activity of **19f** was consistent with the corresponding optical isomers **19g** and **19h**.

Compounds **19a**, **19e**, and **19f** were selected to evaluate preliminary pharmacokinetic (PK) properties in mice following intravenous (iv) and oral (po) administration (Table 5). The AUC and oral bioavailability of **19a** and **19e** were low. The possible reason was that **19a** and **19e** were poorly absorbed in mice. **19f** exhibited favorable drug characteristics with low plasma clearance (CL = 4.1 mL min⁻¹ kg⁻¹), excellent drug exposure (AUC_{0–t} = 49 744 h·ng/L), and oral bioavailability (*F* = 60.4%) using 20 mg/kg oral administration. In addition, compound **19f** also showed good distribution in liver exposure, which was 5950 ng/g after 8 h by oral administration (see

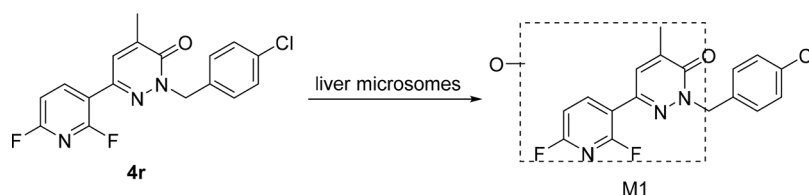


Figure 2. Proposed metabolic pathway of **4r** in liver microsomes.

Supporting Information, Figure S4), being 4-fold higher than that in plasma. Higher liver concentrations of **19f** may be beneficial and reduce the side effects present in chronic HBV infections. As compared with **19a**, the introduction of the polar hydroxyl groups may increase solubility and absorption to improve the oral bioavailability.

In vitro, the anti-HBV activities of **10m**, **19a**, and **19f** were further examined using HepG2.2.15, which stably replicates HBV. HepG2.2.15 cells were treated with **10m**, **19a**, or **19f** at different concentrations for 8 days, and various replication intermediates were extracted and analyzed by Southern blotting. Southern blotting analyses showed that all three compounds inhibited the various forms (relaxed circular [rc] and single-stranded [ss] HBV DNA) in a dose-dependent manner. When compared with compounds **10m** and **19a**, **19f** showed the most potent anti-HBV activity and inhibited the various forms (rcDNA and ssDNA) with lower concentrations (Figure 3). Subsequently, the effect of **19f** on HBV capsid assembly was analyzed. We detected capsid electrophoresis mobility and capsid-associated HBV DNA levels *in situ* on a 1.8% native agarose gel. A type of faster-migrating capsids was detected in **19f** treated samples, which were judged by their mobility on agarose gel as compared to capsids formed in untreated cells (Figure 4, top panel). *In situ* detection of the capsid-associated DNAs was performed by the transfer of HBV capsids onto a nylon sheet, followed by the disruption of capsids and the hybridization with DIG-labeled HBV-specific DNA probe. The treatment of **19f** could reduce capsid-associated DNAs dose-dependently (Figure 4, bottom panel). Notably, no HBV DNA was detected in the faster-migrating capsids. These results revealed that compound **19f** could induce the formation of genome-free capsids, including a phenotype of faster-migrating ones. We also compared the activity of **19f** with other better-studied classes of capsid assembly modulators (CAMs), such as AT-130²⁵ and Bay 41-4109.²⁶ Phenylpropanamide (PPA) derivative AT-130, blocking RNA packaging, showed activity similar to that seen with **19f** treatment on capsid assembly. Heteroaryl-dihydropyrimidines (HAP), Bay 41-4109, effectively reduced the amount of HBV capsids and core-associated genome by stabilizing noncapsid polymers. In contrast, ETV, a well-characterized nucleos(t)ide drug used to treat chronic HBV infections, did not affect HBV capsid formation but, as expected, efficiently inhibited the amount of capsid-associated DNA.

19f with appropriate anti-HBV potency and improved pharmacokinetic (PK) properties was further assessed against HBV infection *in vivo*. An AAV8-HBV-transduced Balb/c mice model was used to determine whether **19f** was effectively delivered via oral administration to exert an antiviral effect on HBV-expressing hepatocytes. Eight-week-old Balb/c male mice received a single tail vein injection with a recombinant adeno-associated virus (AAV) carrying a replicable HBV genome (1×10^{11} viral genome equivalents). After 5 weeks postinjection,

4 groups of 5 mice with stable viremia each were treated with 50 mg/kg **19f** or 150 mg/kg **19f** twice a day (b.i.d.) and 0.5% CMC-Na (vehicle) or 0.1 mg/kg ETV (positive control) once daily (qd) for 4 weeks. Finally, a 4-week treatment regimen with **19f** in this model resulted in a dose-responsive reduction of the HBV DNA level in plasma at the dosages of 50 and 150 mg/kg b.i.d. tested. In comparison to the vehicle-treated control group (0.5% CMC-Na), treatment with 150 mg/kg of **19f** achieved 2.67 log viral load reduction on week 4. Entecavir (ETV), a polymerase inhibitor, was used as a positive control and potentially decreased the amount of HBV DNA in a specific manner (Figure 5). We also evaluated the antiviral activity of **19f** at the dosage of 100 mg/kg b.i.d. in Supporting Information (Figure S5) and showed the significant activity *in vivo*.

Chemistry. To optimize **4r**, analogues described herein were mostly prepared according to the procedure shown in Schemes 1 and 2. First, 4-chloropyridazinone/phthalazinone **8** was prepared by 3,6-dichloropyridazine derivatives **7** refluxing in glacial acetic acid or commercially available pyrazinones **11**, **16**, pyridinone **14**, followed by treatment with 1-chloro-4-(chloromethyl)benzene in the presence of cesium carbonate in DMF to produce the key intermediates **9**, **13**, **15**, **17**, respectively. Afterward, Suzuki cross-coupling with boronic acids yielded the final compounds (Scheme 1). Then, 2,6-difluoropyridine derivative **10m** underwent nucleophilic substitution with alcohol or the corresponding substituted amines to provide **18f–18n** in good yield. Finally, the target compounds **19a–19h** were obtained through introduction of chlorine at the *ortho*-position of aniline of pyridine moiety by *N*-chlorosuccinimide (Scheme 2).

CONCLUSION

In summary, due to the poor pharmacokinetic (PK) properties present in compound **4r**, we described the further optimization based on metabolic pathways, resulting in the discovery of **19f**, a novel phthalazinone derivative with appropriate anti-HBV potencies and improved pharmacokinetic (PK) properties. In *in vitro* studies, **19f** inhibited HBV DNA replication in HepG2.2.15 cells with an IC_{50} of $0.014 \pm 0.004 \mu\text{M}$ and induced the formation of genome-free capsids. In *in vivo* studies, oral administration of **19f** b.i.d. demonstrated a significant reduction of viral DNA at 50, 100, and 150 mg/kg in mice transduced with a recombinant AAV-HBV virus and showed a 2.67 log drop in viral load at 150 mg/kg. On the basis of these results, we identified the novel phthalazinone derivatives that can be effective in both *in vitro* and *in vivo* activities with suitable druggability. The further modification and evaluation of phthalazinone derivatives are ongoing for the development of drug candidate as an oral anti-HBV infection agent.

Table 3. SAR Study on the A-Ring

ID	Structure	CC ₅₀ (μM) ^a	IC ₅₀ (μM) ^b	ID	Structure	CC ₅₀ (μM) ^a	IC ₅₀ (μM) ^b
4r		83.8±11.3	0.098±0.024	10h		31.0±1.72	1.45±0.16
10a		>100	0.17±0.01	10i		>100	NA
10b		>100	NA ^c	10j		90.8±0.2	5.45±2.62
10c		>100	NA	10k		>100	1.89±0.98
10d		92.2±0.13	NA	10l		36.7±5.7	0.33±0.06
10e		39.8±0.24	35.1±2.53	10m		>100	0.12±0.02
10f		56.7±1.35	11.3±0.61	Bay41-4109		>5	0.042±0.010
10g		52.9±7.31	1.22±0.11	AT-130		>20	0.87±0.12

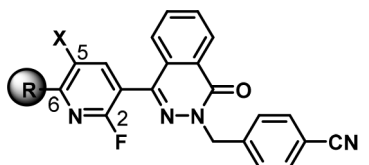
^aCC₅₀ is 50% cytotoxicity concentration in HepG2 2.2.15 cells. ^bIC₅₀ is 50% inhibitory concentration of cytoplasmic HBV-DNA replication. The CC₅₀ and IC₅₀ values are the averages and standard deviations (SD) derived from at least two independent determinations. ^cNA, not active at concentration of CC₅₀.

EXPERIMENTAL SECTION

Synthetic Materials and Methods. All commercially available starting materials and solvents were reagent grade and used without further purification unless otherwise noted. All of the intermediates and final compounds were purified by silica gel (200–300 mesh) chromatography using Biotage SP1 system. ¹H NMR and ¹³C NMR spectral data were recorded in CDCl₃, D₂O, methanol-*d*₄ on a Bruker-600, Bruker-500, Bruker-400, or Varian 300 spectrometer. Data for

NMR spectra were reported as follows: chemical shift (δ ppm), multiplicity integration (s = singlet, brs = broad singlet, d = doublet, t = triplet, q = quartet, dd = doublet of doublets, m = multiplet), coupling constant (Hz). The purities of all the final derivatives for biological testing were confirmed to be >95%, as determined using an Agilent 1260 series HPLC instrument (Agilent Eclipse XBD-C18, 5 μ m, 4.6 mm \times 150 mm, 30 $^{\circ}$ C, UV 254 nm, injection volume = 3 μ L, flow rate = 0.7 mL/min) with aqueous CH₃OH for 25 min. HR-MS was measured on a Micromass Ultra Q-ToF, and ESI-MS was carried

Table 4. SAR Study of Substituents on the Pyridine Moiety



ID	R	X	CC ₅₀ (μM) ^a	IC ₅₀ (μM) ^b	IC ₉₀ (μM) ^c
18a	H ₃ C-	H	>100	0.82±0.09	>10
18b	H ₂ N-	H	>100	0.80±0.04	>10
18c		H	>100	NA ^d	NA
18d		H	>100	0.54±0.07	>10
18e		H	79.2	0.53±0.50	>10
18f		H	>100	2.11±0.02	>10
18g		H	>100	0.43±0.06	>10
19a		Cl	>100	0.038±0.024	0.35±0.04
19b		Cl	9.76±0.84	0.26±0.12	0.87±0.57
19c		Cl	>100	0.21±0.07	1.14±0.07
19d		Cl	>100	0.26±0.01	4.02±0.03
19e		Cl	32.14±2.23	0.028±0.001	0.23±0.002
19f		Cl	>100	0.014±0.004	0.39±0.27
19g		Cl	>100	0.022±0.002	1.01±0.01
19h		Cl	>100	0.008±0.001	0.24±0.06

^aCC₅₀ is 50% cytotoxicity concentration in HepG2 2.2.15 cells. ^bIC₅₀ is 50% inhibitory concentration of cytoplasmic HBV-DNA replication. ^cIC₉₀ is 90% inhibitory concentration of cytoplasmic HBV-DNA replication. The CC₅₀, IC₅₀, and IC₉₀ values are the averages and standard deviations (SDs) derived from at least two independent determinations. ^dNA, not active at concentration of CC₅₀.

out on an Agilent 1260 mass spectrometer (Agilent Technologies, Santa Clara, CA). Optical rotation was measured using a Rudolph Autopol V automatic polarimeter at a wavelength of 589 nm. The preparations of compounds 10c–10h, 10l–10m, 18a–18g, 19a–19h

Table 5. Single-Dose Pharmacokinetics of Selected Compounds in Mice^a

compd	dose (mg/kg)	T _{1/2} (h)	T _{max} (h)	C _{max} (ng/mL)	AUC _{0–t} (h·ng/mL)	AUC _{INF_obs} (h·ng/mL)	Cl _{obs} (mL min ⁻¹ kg ⁻¹)	Vss (mL/kg)	F (%)
19a	20 (po)	3.83 ± 0.82	2.33 ± 1.53	94.8 ± 25.5	835 ± 208	850 ± 210			2.7
	2 (iv)	3.09 ± 0.88			3047 ± 494	3073 ± 525	11.1 ± 1.96	3088 ± 356	
19e	20 (po)		1 ± 0.29	69.5 ± 36.4	115 ± 63	171 ± 102			1.9
	2 (iv)		0.25		604 ± 108	735 ± 150	2720.2 ± 823.5	5444 ± 1250	
19f	20 (po)	2.15 ± 0.02	1.33 ± 0.58	9670 ± 3324	49744 ± 20791	49778 ± 20810			60.4
	2 (iv)	2.52 ± 0.14			8241 ± 615	8251 ± 612	4.1 ± 0.3	766 ± 123	

^aSingle-dose pharmacokinetics (SDPK) studies of selected compounds were carried out in mice according to standard procedures. The major parameters, including half-life (T_{1/2}), T_{max}, maximal concentration (C_{max}), the area under the curve (AUC_{0–t}, AUC_{INF_obs}), plasma clearance (Cl_{obs}), volume of distribution at steady state (Vss), and oral bioavailability (F), were reported.

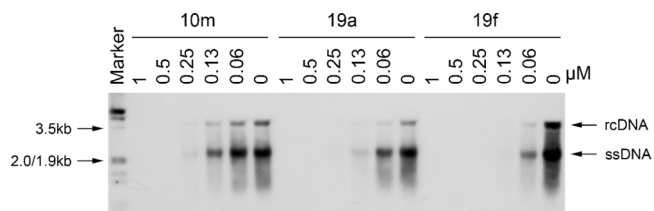


Figure 3. 10m, 19a, and 19f inhibited HBV DNA replication *in vitro*. HepG2.2.15 cells were treated with 10m, 19a, or 19f at the indicated concentrations for 8 days. HBV replication intermediates were detected by Southern blotting hybridization using a DIG-labeled HBV genomic fragment as a probe. All three compounds inhibited the various forms in a dose-dependent manner, and 19f specifically decreased the amount of intracellular HBV DNA with lower concentrations. rcDNA is relaxed circular HBV DNA. ssDNA is single-stranded HBV DNA.

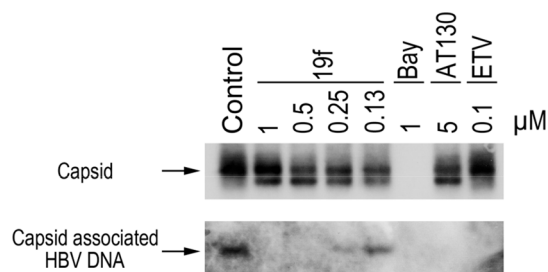


Figure 4. 19f induced the formation of HBV DNA-free capsids. HepG2.2.15 cells were treated with 19f at the indicated concentrations for 8 days. Capsids were analyzed on 1.8% agarose gel (top panel). Capsid-associated HBV DNA was detected by the transfer of HBV capsids on a nylon sheet, followed by Southern blotting hybridization upon disruption of capsids *in situ* (bottom panel). Compound 19f treatment led to an accumulation of faster-migrating capsid. The levels of HBV DNA packaged in capsid with the same electrophoresis mobility as the control were decreased by 19f treatment in a dose-dependent manner.

were described below, while the experimental procedures of 10a–10b, 10i–10k, and key intermediates were provided in the Supporting Information.

2-(4-Chlorobenzyl)-6-(2,6-difluoropyridin-3-yl)-4-(hydroxymethyl)pyridazin-3(2H)-one (10a). The synthetic procedure was described in the Supporting Information. White solid (77% yield); mp 114.4–115.1 °C; ¹H NMR (400 MHz, chloroform-*d*) δ 8.37–8.29 (m, 1H), 7.76 (brs, 1H), 7.43 (d, *J* = 8.2 Hz, 2H), 7.34 (d, *J* = 8.2 Hz, 2H), 7.00 (dd, *J* = 8.2, 3.0 Hz, 1H), 5.39 (s, 2H), 4.73 (d, *J* = 4.7 Hz, 2H), 2.82 (s, 1H).

2-(4-Chlorobenzyl)-6-(2,6-difluoropyridin-3-yl)-3-oxo-2,3-dihydropyridazine-4-carboxylic Acid (10b). The synthetic procedure was described in the Supporting Information. White solid

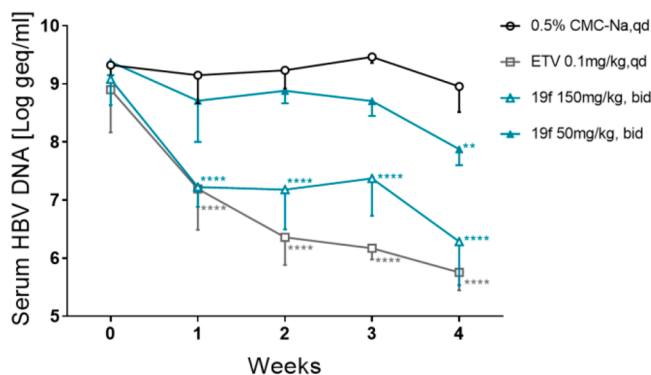


Figure 5. Levels of HBV DNA in the plasma of AAV/HBV-infected mice by treatment of **19f** with 50 mg/kg and 150 mg/kg, b.i.d. After 4 weeks treatment, oral administration of **19f** (b.i.d.) demonstrates a statistically significant reduction of the HBV DNA level of up to 2.67 log at 150 mg/kg in mice transduced with a recombinant AAV-HBV virus compared to that in the vehicle-treated control mice (Dunnett's multiple comparisons test, $P < 0.0001$). The treatment regimen with 50 mg/kg **19f** resulted in a 1.08 log reduction of the HBV DNA viral load ($P < 0.01$). Data were shown as the mean \pm SD. The number of animals per group for data analysis was 5.

(67% yield); mp 216.2–216.8 °C; ^1H NMR (400 MHz, chloroform-*d*) δ 13.63 (s, 1H), 8.67 (brs, 1H), 8.35–8.28 (m, 1H), 7.47 (d, $J = 8.2$ Hz, 2H), 7.38 (d, $J = 8.2$ Hz, 2H), 7.06 (dd, $J = 8.2, 3.0$ Hz, 1H), 5.51 (s, 2H).

General Procedure A for the Synthesis of 10c–10h, 10l, 10m. 3,6-Dichloropyridazine-4-carboxylic acid **7** (10.0 g, 51.8 mmol) was placed in AcOH (100 mL) and stirred for 4 h at refluxing. After cooling, the reaction mixture was poured into water and a white solid was precipitated, filtered, washed with water, and dried to afford 6-chloro-3-oxo-2,3-dihydropyridazine-4-carboxylic acid (6.7 g, 75%).

To a solution of 6-chloro-3-oxo-2,3-dihydropyridazine-4-carboxylic acid (4.8 g, 27.5 mmol) in MeOH (100 mL) was added HCl (30 mL, 4 M in dioxane), and the mixture was stirred for 20 h at 50 °C. After the reaction was finished, the solvent was removed under reduced pressure. The residue was diluted with water (20 mL), extracted with ethyl acetate (15 mL \times 3) and the combined organic layers were washed with brine (10 mL), dried over anhydrous Na_2SO_4 , filtered, and concentrated to give the crude product, which was purified by column chromatography ($\text{CH}_2\text{Cl}_2/\text{MeOH} = 20/1$, v/v) to afford methyl 6-chloro-3-oxo-2,3-dihydropyridazine-4-carboxylate (4.5 g, 86%).

To a solution of methyl 6-chloro-3-oxo-2,3-dihydropyridazine-4-carboxylate (4.0 g, 21.2 mmol) in DMF (100 mL) were added Cs_2CO_3 (7.6 g, 23.3 mmol) and 1-chloro-4-(chloromethyl)benzene (3.8 g, 23.3 mmol). The resulting mixture was stirred at 50 °C for 7 h, then the solvent was removed under reduced pressure. The residue was diluted with water (100 mL), extracted with ethyl acetate (50 mL \times 3) and the combined organic layers were washed with brine (100 mL), dried over anhydrous Na_2SO_4 , filtered, and concentrated to give the crude product, which was further purified by column chromatography on silica gel eluting with 25% ethyl acetate in hexane to give the desired product **9c** (5.05 g, 76%). ^1H NMR (400 MHz, chloroform-*d*) δ 7.73 (s, 1H), 7.42 (d, $J = 8.1$ Hz, 3H), 7.30 (d, $J = 8.4$ Hz, 3H), 5.24 (s, 3H), 3.93 (s, 9H).

To a three-necked round-bottom flask was added **9c** (50 mg, 0.16 mmol), $\text{Pd}(\text{OAc})_2$ (1.79 mg, 0.016 mmol, 0.05 equiv), X-Phos (7.61 mg, 0.032 mmol, 0.1equiv), potassium carbonate (44 mg, 0.32 mmol, 2.0 equiv) under the atmosphere of nitrogen, followed by adding the combined solution of tetrahydrofuran (4 mL) and water (1 mL). Then a solution of (2,6-difluoropyridin-3-yl)boronic acid (30 mg, 0.19 mmol, 1.2 equiv) in THF (1 mL) was added dropwise. The resulting mixture was stirred at 60 °C for 2 h. After cooling, the reaction mixture was filtered and the filtrate was extracted with ethyl acetate (15 mL \times 3) and the combined organic layers were washed

with brine (10 mL), dried over anhydrous Na_2SO_4 , filtered, and concentrated to give the crude product, which was further purified by column chromatography to afford methyl-2-(4-chlorobenzyl)-6-(2,6-difluoropyridin-3-yl)-3-oxo-2,3-dihydropyridazine-4-carboxylate (**10c**). White solid (47.5 mg, 76% yield); mp 148.2–148.7 °C; ^1H NMR (400 MHz, chloroform-*d*) δ 8.37–8.31 (m, 1H), 8.27 (d, $J = 1.7$ Hz, 1H), 7.46 (d, $J = 8.4$ Hz, 2H), 7.33 (d, $J = 8.4$ Hz, 2H), 7.02 (dd, $J = 8.2, 3.0$ Hz, 1H), 5.41 (s, 2H), 3.98 (s, 3H).

2-(4-Chlorobenzyl)-6-(2,6-difluoropyridin-3-yl)-4-methoxy-pyridazin-3(2H)-one (10d). This compound was prepared by replacement of 3,6-dichloropyridazine-4-carboxylic acid with 3,6-dichloro-4-methoxy-1,2-dihydropyridazine using a similar synthetic procedure A. White solid (73% yield); mp 125.6–126.0 °C; ^1H NMR (400 MHz, chloroform-*d*) δ 8.39–8.31 (m, 1H), 7.44 (d, $J = 8.4$ Hz, 2H), 7.31 (d, $J = 8.4$ Hz, 2H), 6.98 (dd, $J = 8.2, 3.0$ Hz, 1H), 6.92 (s, 1H), 5.39 (s, 2H), 3.96 (s, 3H).

2-(4-Chlorobenzyl)-4-cyclopropyl-6-(2,6-difluoropyridin-3-yl)pyridazin-3(2H)-one (10e). This compound was prepared by replacement of 3,6-dichloropyridazine-4-carboxylic acid with 3,6-dichloro-4-cyclopropyl-1,2-dihydropyridazine using a similar synthetic procedure A. White solid (64% yield); mp 57.5–58.3 °C. ^1H NMR (400 MHz, chloroform-*d*) δ 8.36–8.26 (m, 1H), 7.45 ($J = 8.3$ Hz, 2H), 7.33 (d, $J = 8.3$ Hz, 2H), 7.09 (brs, 1H), 6.97 (dd, $J = 8.2, 3.0$ Hz, 1H), 5.38 (s, 2H), 2.39–2.31 (m, 1H), 1.22–1.15 (m, 2H), 0.91–0.84 (m, 2H).

2-(4-Chlorobenzyl)-6-(2,6-difluoropyridin-3-yl)-4-isopropyl-pyridazin-3(2H)-one (10f). This compound was prepared by replacement of 3,6-dichloropyridazine-4-carboxylic acid with 3,6-dichloro-4-isopropyl-1,2-dihydropyridazine using a similar synthetic procedure A. White solid (69% yield); mp 62.5–63.2 °C; ^1H NMR (400 MHz, chloroform-*d*) δ 8.35–8.29 (m, 1H), 7.49–7.48 (m, 1H), 7.44 ($J = 8.3$ Hz, 2H), 7.33 ($J = 8.3$ Hz, 2H), 7.00–6.97 (m, 1H), 5.38 (s, 2H), 3.33–3.22 (m, 1H), 1.27 (s, 3H), 1.25 (s, 3H).

2-(4-Chlorobenzyl)-6-(2,6-difluoropyridin-3-yl)-4,5-dimethylpyridazin-3(2H)-one (10g). This compound was prepared by replacement of 3,6-dichloropyridazine-4-carboxylic acid with 3,6-dichloro-4,5-dimethyl-1,2-dihydropyridazine using a similar synthetic procedure A. White solid (71% yield); mp 87.2–87.8 °C; ^1H NMR (400 MHz, chloroform-*d*) δ 7.94–7.81 (m, 1H), 7.41 (d, $J = 8.4$ Hz, 2H), 7.31 (d, $J = 8.4$ Hz, 2H), 6.99 (dd, $J = 8.0, 2.8$ Hz, 1H), 5.31 (s, 2H), 2.24 (s, 3H), 2.06 (s, 3H).

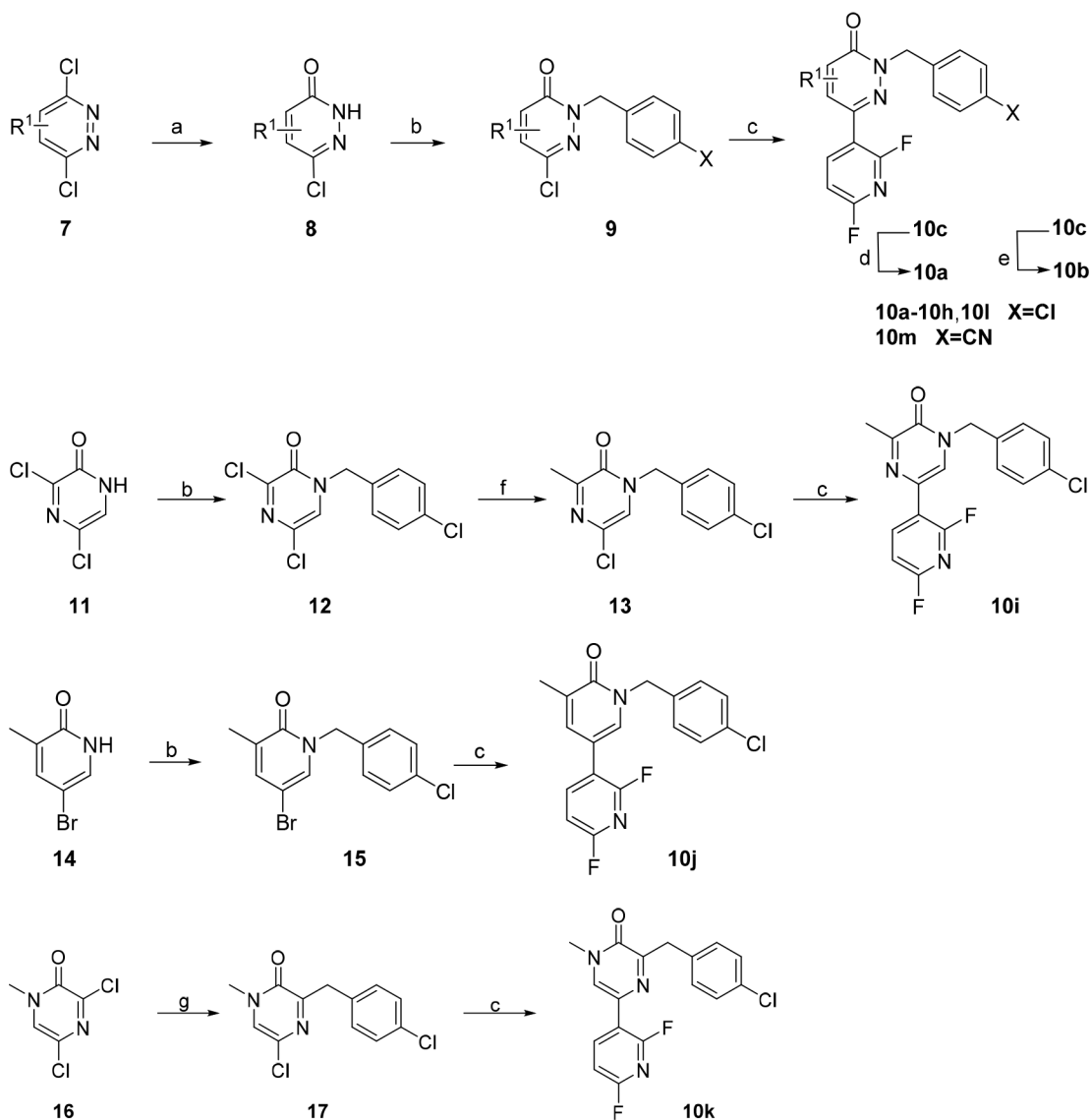
2-(4-Chlorobenzyl)-4-(2,6-difluoropyridin-3-yl)-5,6,7,8-tetrahydrophthalazin-1(2H)-one (10h). This compound was prepared by replacement of 3,6-dichloropyridazine-4-carboxylic acid with 1,4-dichloro-2,3,5,6,7,8-hexahydrophthalazine using a similar synthetic procedure A. White solid (72% yield); mp 114.2–114.6 °C; ^1H NMR (300 MHz, deuterium oxide) δ 7.89–7.81 (m, 1H), 7.40 (d, $J = 8.3$ Hz, 2H), 7.29 (d, $J = 8.3$ Hz, 2H), 6.96 (d, $J = 8.0$ Hz, 1H), 5.28 (s, 2H), 2.65–2.61 (m, 2H), 2.32–2.30 (m, 2H), 1.81–1.66 (m, 4H).

1-(4-Chlorobenzyl)-5-(2,6-difluoropyridin-3-yl)-3-methylpyrazin-2(1H)-one (10i). The synthetic procedure was described in the Supporting Information. White solid (68% yield); mp 116.7–117.3 °C; ^1H NMR (400 MHz, chloroform-*d*) δ 8.03–7.90 (m, 1H), 7.57 (d, $J = 8.0$ Hz, 2H), 7.46 (d, $J = 8.0$ Hz, 2H), 7.16 (s, 1H), 6.97 (dd, $J = 8.0, 2.8$ Hz, 1H), 5.12 (s, 2H), 2.53 (s, 3H).

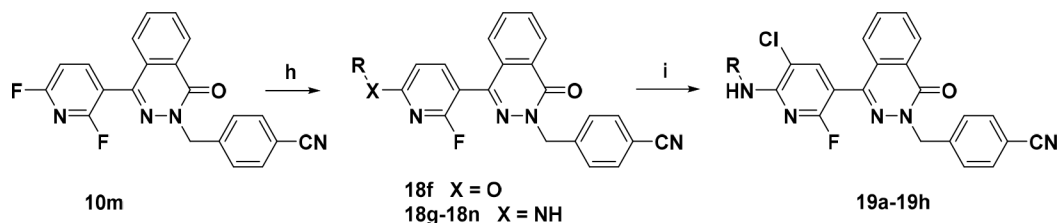
1-(4-Chlorobenzyl)-2',6'-difluoro-5-methyl-[3,3'-bipyridin]-6(1H)-one (10j). The synthetic procedure was described in the Supporting Information. White solid (75% yield); mp 119.8–120.2 °C; ^1H NMR (400 MHz, chloroform-*d*) δ 7.88–7.82 (m, 1H), 7.48–7.46 (m, 1H), 7.41–7.39 (m, 1H), 7.37–7.30 (m, 3H), 6.92 (dd, $J = 8.1, 3.0$ Hz, 1H), 5.19 (s, 2H), 2.26 (s, 3H).

3-(4-Chlorobenzyl)-5-(2,6-difluoropyridin-3-yl)-1-methylpyrazin-2(1H)-one (10k). The synthetic procedure was described in the Supporting Information. White solid (66% yield); mp 190.7–191.2 °C; ^1H NMR (400 MHz, chloroform-*d*) δ 8.60–8.51 (m, 1H), 7.82 (s, 1H), 7.63 (d, $J = 8.0$ Hz, 2H), 7.54 (d, $J = 8.0$ Hz, 2H), 6.98 (dd, $J = 8.4, 3.0$ Hz, 1H), 4.28 (s, 2H), 3.64 (s, 3H).

2-(4-Chlorobenzyl)-4-(2,6-difluoropyridin-3-yl)phthalazin-1(2H)-one (10l). This compound was prepared by replacement of 3,6-dichloropyridazine-4-carboxylic acid with 1,4-dichloro-2,3-dihy-

Scheme 1. Synthesis of 10a–10m^a

^aReagents and conditions: (a) AcOH, reflux; (b) 1-chloro-4-(chloromethyl)benzene/4-(chloromethyl)benzonitrile, Cs₂CO₃, DMF, 50 °C; (c) boronic acids, Pd(OAc)₂, X-Phos, K₂CO₃, THF/H₂O, 60 °C; (d) DIBAL-H, toluene, −10 °C; (e) LiOH, THF/H₂O, rt; (f) tetramethyltin, Pd(PPh₃)₄, toluene, reflux; (g) 1-chloro-4-(chloromethyl)benzene, Bu₃SnSnBu₃, Pd(PPh₃)₄, DMF, microwave, 170 °C.

Scheme 2. Synthesis of 18f–18n and 19a–19h^a

^aReagents and conditions: (h) CH₃CH₂OH, NaH, THF, 0 °C or RNH₂, K₂CO₃, DMSO, 70 °C, 3 h; (i) NCS, CH₃CN/THF, reflux 3 h.

drophthalazine using a similar synthetic procedure A. White solid (78% yield); mp 125.3–125.9 °C; ¹H NMR (400 MHz, chloroform-*d*) δ 8.53–8.49 (m, 1H), 8.07–7.99 (m, 1H), 7.83–7.75 (m, 2H), 7.45–7.39 (m, 3H), 7.31–7.26 (m, 2H), 7.03 (dd, *J* = 8.0, 2.6 Hz, 1H), 5.40 (s, 2H). ¹³C NMR (126 MHz, chloroform-*d*) δ 162.53 (d, *J* = 14.8 Hz), 160.54 (d, *J* = 14.7 Hz), 159.37 (d, *J* = 15.1 Hz), 158.41, 157.39 (d, *J* = 15.1 Hz), 146.23 (dd, *J* = 7.9, 3.9 Hz), 139.55 (d, *J* = 4.1 Hz), 134.48, 133.34, 132.91, 131.57, 129.68, 128.30, 128.26,

127.48, 126.96, 125.06 (d, *J* = 2.5 Hz), 114.20 (dd, *J* = 28.0, 6.4 Hz), 106.38 (dd, *J* = 34.5, 5.9 Hz), 53.91. HRMS (ESI): exact mass calcd for C₂₀H₁₃ClF₂N₃O⁺ [M + H]⁺, 384.0715; found, 384.0710. HPLC purity 98.3% (*t*_R = 19.35 min).

4-((4-(2,6-Difluoropyridin-3-yl)-1-oxophthalazin-2(1H)-yl)-methyl)benzonitrile (10m). This compound was prepared by replacement of 1-chloro-4-(chloromethyl)benzene with 4-(chloromethyl)benzonitrile in a similar manner to 10l. White solid

(73% yield); mp 181.5–182.3 °C; ^1H NMR (400 MHz, chloroform-*d*) δ 8.57–8.52 (m, 1H), 8.08–8.02 (m, 1H), 7.89–7.81 (m, 2H), 7.68–7.63 (m, 2H), 7.62–7.57 (m, 2H), 7.48–7.43 (m, 1H), 7.07 (dd, $J = 8.1, 2.8$, 1H), 5.50 (s, 2H). ^{13}C NMR (126 MHz, chloroform-*d*) δ 163.10 (d, $J = 14.4$ Hz), 161.10 (d, $J = 14.6$ Hz), 159.88 (d, $J = 13.9$ Hz), 158.99, 157.90 (d, $J = 13.8$ Hz), 146.62 (dd, $J = 8.1, 3.8$ Hz), 141.62, 140.48 (d, $J = 4.2$ Hz), 133.65, 132.46, 132.29, 129.27, 128.83, 127.87, 127.49, 125.70 (d, $J = 2.3$ Hz), 118.60, 114.49 (d, $J = 22.1$ Hz), 111.86, 106.92 (dd, $J = 34.6, 5.7$ Hz), 54.65. HRMS (ESI): exact mass calcd for $\text{C}_{21}\text{H}_{12}\text{F}_2\text{N}_4\text{O}_2\text{Na}^+ [\text{M} + \text{Na}]^+$, 397.0877; found, 397.0875. HPLC purity 98.5% ($t_{\text{R}} = 10.10$ min).

4-((4-(2-Fluoro-6-methylpyridin-3-yl)-1-oxophthalazin-2(1H)-yl)methyl)benzotrile (18a). This compound (a white solid) was prepared by replacement of (2,6-difluoropyridin-3-yl)boronic acid with (2-fluoro-6-methylpyridin-3-yl)boronic acid using a similar synthetic procedure A. White solid (78% yield); mp 180.8–181.2 °C; ^1H NMR (300 MHz, deuterium oxide) δ 8.52–8.48 (m, 1H), 7.85–7.76 (m, 3H), 7.63 (d, $J = 8.5$ Hz, 2H), 7.57 (d, $J = 8.5$ Hz, 2H), 7.49–7.44 (m, 1H), 7.24–7.21 (m, 1H), 5.48 (s, 2H), 2.63 (s, 3H). ^{13}C NMR (126 MHz, chloroform-*d*) δ 160.48, 159.05, 158.94, 158.58, 141.95 (d, $J = 3.7$ Hz), 141.30, 141.25 (d, $J = 4.6$ Hz), 132.96, 131.92, 131.57, 128.74, 128.58, 127.33, 126.79, 125.58, 120.67 (d, $J = 4.4$ Hz), 118.16, 113.88, 113.63, 111.25, 54.11, 23.41. HRMS (ESI): exact mass calcd for $\text{C}_{22}\text{H}_{16}\text{FN}_4\text{O}^+ [\text{M} + \text{H}]^+$, 371.1308; found, 371.1303. HPLC purity 99.6% ($t_{\text{R}} = 13.76$ min).

4-((4-(6-Amino-2-fluoropyridin-3-yl)-1-oxophthalazin-2(1H)-yl)methyl)benzotrile (18b). This compound (a white solid) was prepared by replacement of (2,6-difluoropyridin-3-yl)boronic acid with (6-amino-2-fluoropyridin-3-yl)boronic acid using a similar synthetic procedure A. White solid (71% yield); mp 243.2–243.7 °C; ^1H NMR (400 MHz, chloroform-*d*) δ 8.54–8.49 (m, 1H), 7.85–7.78 (m, 2H), 7.69–7.55 (m, 6H), 6.52 (dd, $J = 8.0, 1.8$ Hz, 1H), 5.50 (s, 2H), 4.81 (s, 2H). ^{13}C NMR (126 MHz, chloroform-*d*) δ 160.68, 158.78, 158.64, 158.00, 157.86, 143.00 (d, $J = 4.4$ Hz), 141.93, 141.50, 132.78, 131.89, 131.34, 128.99, 128.69, 127.37, 126.67, 125.94, 118.22, 111.14, 104.57 (d, $J = 4.6$ Hz), 104.37, 54.06. HRMS (ESI): exact mass calcd for $\text{C}_{21}\text{H}_{15}\text{FN}_5\text{O}^+ [\text{M} + \text{H}]^+$, 372.1261; found, 372.1253. HPLC purity 96.3% ($t_{\text{R}} = 11.48$ min).

N-(5-(3-(4-Cyanobenzyl)-4-oxo-3,4-dihydrophthalazin-1-yl)-6-fluoropyridin-2-yl)acetamide (18c). To a solution of 18b (185 mg, 0.50 mmol) in anhydrous pyridine (2.2 mL) cooled to 0 °C was slowly added acetic anhydride (0.50 mL, 5.5 mmol). After addition was complete, the reaction was allowed to warm to room temperature and stir overnight. After an aqueous sodium bicarbonate workup with ethyl acetate extraction, the organic layers were pooled and concentrated to give an oil which was purified by silica gel chromatography with 50% ethyl acetate in hexanes to give the desired product 18c (177 mg, 86%). White solid (76% yield); mp 249.1–249.8 °C; ^1H NMR (400 MHz, chloroform-*d*) δ 8.54–7.52 (m, 1H), 8.29–7.27 (m, 1H), 7.97–7.92 (m, 1H), 7.86–7.80 (m, 2H), 7.65 (d, $J = 8.3$ Hz, 2H), 7.60 (d, $J = 8.3$ Hz, 2H), 7.50–7.47 (m, 1H), 5.51 (s, 2H), 2.30 (s, 3H).

General Procedure B for the Synthesis of 18d, 18e, 18g. A mixture of halogenated pyridine 10m (1.0 mmol), amine (1.0 equiv), and K_2CO_3 (1.3 equiv) in DMSO (5 mL) was allowed to react under air atmosphere. The reaction mixture was heated to 70 °C for 2 h. After reaction, the reaction mixture was added to brine (15 mL) and extracted with ethyl acetate (15 mL \times 3). The solvent was concentrated under vacuum, and the product was isolated by short chromatography on a silica gel (200–300 mesh) column.

4-((4-(2-Fluoro-6-(methylamino)pyridin-3-yl)-1-oxophthalazin-2(1H)-yl)methyl)benzotrile (18d). White solid (71% yield); mp 222.8–223.4 °C; ^1H NMR (400 MHz, chloroform-*d*) δ 8.54–8.47 (m, 1H), 7.85–7.77 (m, 2H), 7.67–7.57 (m, 6H), 6.40 (dd, $J = 8.2, 1.8$ Hz, 1H), 5.50 (s, 2H), 4.96 (s, 1H), 3.03 (d, $J = 5.1$ Hz, 3H). ^{13}C NMR (126 MHz, chloroform-*d*) δ 160.75, 158.99 (d, $J = 17.1$ Hz), 158.85, 158.66, 142.50 (d, $J = 4.4$ Hz), 142.31 (d, $J = 4.5$ Hz), 141.57, 132.71, 131.88, 131.26, 129.12, 128.70, 127.38, 126.60, 126.07 (d, $J = 2.7$ Hz), 123.08, 118.24, 111.09, 102.82 (d, $J = 30.4$

Hz), 102.47, 54.03, 28.52. HRMS (ESI): exact mass calcd for $\text{C}_{22}\text{H}_{17}\text{FN}_5\text{O}^+ [\text{M} + \text{H}]^+$, 386.1417; found, 386.1409. HPLC purity 99.8% ($t_{\text{R}} = 13.36$ min).

4-((4-(6-(Dimethylamino)-2-fluoropyridin-3-yl)-1-oxophthalazin-2(1H)-yl)methyl)benzotrile (18e). White solid (73% yield); mp 182.7–183.2 °C; ^1H NMR (400 MHz, chloroform-*d*) δ 8.56–8.45 (m, 1H), 7.83–7.74 (m, 2H), 7.67–7.56 (m, 6H), 6.48 (dd, $J = 8.4, 2.0$ Hz, 1H), 5.50 (s, 2H), 3.19 (s, 6H). ^{13}C NMR (151 MHz, chloroform-*d*) δ 160.13, 158.74, 158.55, 158.44, 142.60, 142.30 (d, $J = 4.4$ Hz), 141.66, 132.74, 131.94, 131.28, 129.24, 128.78, 127.42, 126.62, 126.23, 118.35, 111.10, 102.02 (d, $J = 3.8$ Hz), 101.54, 101.33, 54.07, 37.68, 24.43. HRMS (ESI): exact mass calcd for $\text{C}_{23}\text{H}_{19}\text{FN}_5\text{O}^+ [\text{M} + \text{H}]^+$, 400.1574; found, 400.1570. HPLC purity 98.8% ($t_{\text{R}} = 15.72$ min).

4-((4-(6-Ethoxy-2-fluoropyridin-3-yl)-1-oxophthalazin-2(1H)-yl)methyl)benzotrile (18f). Ethanol (42 μL , 0.53 mmol) was added to a suspension of NaH (16 mg, 0.53 mmol, 60% in mineral oil) in anhydrous THF (5 mL). After 10 min, a solution of 10m (100 mg, 0.27 mmol) in THF was added at 0 °C. The reaction was then warmed to room temperature and stirred at ambient temperature overnight, quenched with water, extracted with ethyl acetate (15 mL \times 3). The solvent was concentrated under vacuum and the product was isolated by short chromatography on a silica gel (200–300 mesh) column eluting with 40% ethyl acetate in hexanes to give the desired product 18f. White solid (78% yield); mp 195.1–195.4 °C; ^1H NMR (400 MHz, chloroform-*d*) δ 8.54–8.50 (m, 1H), 7.86–7.80 (m, 2H), 7.80–7.75 (m, 1H), 7.65 (d, $J = 8.3$ Hz, 2H), 7.60 (d, $J = 8.3$ Hz, 2H), 7.56–7.51 (m, 1H), 6.80 (dd, $J = 8.2, 1.2$ Hz, 1H), 5.50 (s, 2H), 4.45 (q, $J = 7.1$ Hz, 2H), 1.47 (t, $J = 7.1$ Hz, 3H).

4-((4-(2-Fluoro-6-((2-methoxyethyl)amino)pyridin-3-yl)-1-oxophthalazin-2(1H)-yl)methyl)benzotrile (18g). White solid (81% yield); mp 140.0–140.7 °C; ^1H NMR (400 MHz, chloroform-*d*) δ 8.52–8.47 (m, 1H), 7.83–7.76 (m, 2H), 7.67–7.52 (m, 7H), 6.43 (dd, $J = 8.2, 1.8$ Hz, 1H), 5.49 (s, 2H), 5.26 (t, $J = 5.2$ Hz, 1H), 3.72–3.53 (m, 4H), 3.43 (s, 3H). ^{13}C NMR (126 MHz, chloroform-*d*) δ 161.30, 159.41, 159.16, 158.71, 158.57, 142.79 (d, $J = 4.5$ Hz), 142.06, 133.20, 132.38, 131.75, 129.60, 127.89, 127.11, 126.57, 118.74, 111.61, 104.37, 103.46, 103.21, 70.92, 58.87, 54.53, 41.57. HRMS (ESI): exact mass calcd for $\text{C}_{24}\text{H}_{21}\text{FN}_5\text{O}_2^+ [\text{M} + \text{H}]^+$, 430.1679; found, 430.1675. HPLC purity 97.7% ($t_{\text{R}} = 14.19$ min).

General Procedure C for the Synthesis of 19a–19h. 18g (200 mg, 0.46 mmol) was mixed with *N*-chlorosuccinimide (62 mg, 0.46 mmol, 1.0 equiv) in acetonitrile (5 mL) and heated at reflux overnight. The reaction mixture was concentrated with silica gel and purified by column chromatography with 15% ethyl acetate in hexanes to afford 4-((4-(5-chloro-2-fluoro-6-((2-methoxyethyl)amino)pyridin-3-yl)-1-oxophthalazin-2(1H)-yl)methyl)benzotrile (19a) (194 mg, 90% yield); mp 141.2–141.6 °C; ^1H NMR (400 MHz, chloroform-*d*) δ 8.52–8.45 (m, 1H), 7.85–7.77 (m, 2H), 7.66–7.61 (m, 3H), 7.59–7.56 (m, 3H), 5.71 (t, $J = 5.4$ Hz, 1H), 5.47 (s, 2H), 3.76–3.69 (m, 2H), 3.64–3.62 (m, 2H), 3.44 (s, 3H). ^{13}C NMR (126 MHz, chloroform-*d*) δ 159.53, 159.09, 157.63, 153.64 (d, $J = 18.1$ Hz), 141.90, 141.61 (d, $J = 4.7$ Hz), 140.82 (d, $J = 5.1$ Hz), 133.34, 132.41, 131.92, 129.33, 129.20, 127.87, 127.21, 126.34 (d, $J = 2.7$ Hz), 118.70, 111.69, 111.00 (d, $J = 4.9$ Hz), 103.79, 103.53, 70.84, 58.92, 54.62, 41.42. HRMS (ESI): exact mass calcd for $\text{C}_{24}\text{H}_{20}\text{ClFN}_5\text{O}_2^+ [\text{M} + \text{H}]^+$, 464.1290; found, 464.1277. HPLC purity 100% ($t_{\text{R}} = 17.31$ min).

4-((4-(5-Chloro-6-((2-(dimethylamino)ethyl)amino)-2-fluoropyridin-3-yl)-1-oxophthalazin-2(1H)-yl)methyl)benzotrile (19b). White solid (73% yield); mp 104.1–104.5 °C; ^1H NMR (400 MHz, chloroform-*d*) δ 8.52–8.48 (m, 1H), 7.84–7.78 (m, 2H), 7.67–7.62 (m, 3H), 7.62–7.57 (m, 3H), 6.04 (brs, 1H), 5.49 (s, 2H), 3.60–3.55 (m, 2H), 2.62 (t, $J = 6.0$ Hz, 2H), 2.34 (s, 6H). ^{13}C NMR (126 MHz, chloroform-*d*) δ 159.60, 159.10, 157.71, 153.87, 153.73, 141.91, 141.72, 140.60 (d, $J = 5.2$ Hz), 133.31, 132.41, 131.89, 129.36, 129.20, 127.87, 127.20, 126.39, 118.70, 111.68, 111.01 (d, $J = 5.0$ Hz), 103.32, 103.06, 57.64, 54.61, 45.20, 39.02. HRMS (ESI):

exact mass calcd for $C_{25}H_{23}ClFN_6O^+$ $[M + H]^+$, 477.1606; found, 477.1596. HPLC purity 99.5% ($t_R = 12.25$ min).

Methyl 3-((3-Chloro-5-(3-(4-cyanobenzyl)-4-oxo-3,4-dihydrophthalazin-1-yl)-6-fluoropyridin-2-yl)amino)propanoate (19c). White solid (72% yield); mp 157.2–157.7 °C; 1H NMR (400 MHz, chloroform-*d*) δ 8.52–8.45 (m, 1H), 7.83–7.77 (m, 2H), 7.66–7.61 (m, 3H), 7.59–7.54 (m, 3H), 5.91 (t, $J = 6.2$ Hz, 1H), 5.47 (s, 2H), 3.83 (q, $J = 6.0$ Hz, 2H), 3.75 (s, 3H), 2.73 (t, $J = 6.0$ Hz, 2H). ^{13}C NMR (126 MHz, chloroform-*d*) δ 172.84, 159.54, 159.07, 157.64, 153.38 (d, $J = 18.1$ Hz), 141.88, 141.54 (d, $J = 4.7$ Hz), 140.91 (d, $J = 5.0$ Hz), 133.35, 132.41, 131.94, 129.30, 129.20, 127.86, 127.22, 126.32 (d, $J = 2.7$ Hz), 118.69, 111.69, 111.03 (d, $J = 4.8$ Hz), 104.03, 103.76, 54.62, 51.89, 37.14, 33.62. HRMS (ESI): exact mass calcd for $C_{25}H_{20}ClFN_5O_3^+$ $[M + H]^+$, 492.1239; found, 492.1229. HPLC purity 99.4% ($t_R = 17.02$ min).

3-((3-Chloro-5-(3-(4-cyanobenzyl)-4-oxo-3,4-dihydrophthalazin-1-yl)-6-fluoropyridin-2-yl)amino)propanoic Acid (19d). White solid (79% yield); mp 128.3–128.8 °C; 1H NMR (400 MHz, chloroform-*d*) δ 8.53–8.46 (m, 1H), 7.83–7.77 (m, 2H), 7.68–7.60 (m, 3H), 7.59–7.53 (m, 3H), 5.86 (t, $J = 6.4$ Hz, 1H), 5.47 (s, 2H), 3.85 (q, $J = 6.0$ Hz, 2H), 2.80 (t, $J = 6.0$ Hz, 2H). ^{13}C NMR (126 MHz, chloroform-*d*) δ 177.10, 159.38, 157.64, 153.35 (d, $J = 17.9$ Hz), 142.00, 141.68, 140.98 (d, $J = 5.2$ Hz), 133.59, 132.45, 132.16, 129.30, 129.23, 127.68, 127.28, 126.37, 118.62, 111.72, 111.05, 104.10, 103.84, 54.78, 36.93, 33.57. HRMS (ESI): exact mass calcd for $C_{24}H_{18}ClFN_5O_3^+$ $[M + H]^+$, 478.1082; found, 478.1070. HPLC purity 99.0% ($t_R = 14.91$ min).

4-((4-(5-Chloro-2-fluoro-6-((2-hydroxyethyl)amino)pyridin-3-yl)-1-oxophthalazin-2(1H)-yl)methyl)benzoxonitrile (19e). White solid (86% yield); mp 201.2–201.4 °C; 1H NMR (400 MHz, chloroform-*d*) δ 8.52–8.45 (m, 1H), 7.83–7.77 (m, 2H), 7.68–7.60 (m, 3H), 7.60–7.53 (m, 3H), 5.75 (t, $J = 5.8$ Hz, 1H), 5.47 (s, 2H), 3.93–3.88 (m, 2H), 3.73 (q, $J = 5.3$ Hz, 2H), 2.19 (s, 1H). ^{13}C NMR (126 MHz, chloroform-*d*) δ 159.48, 159.10, 157.58, 153.91, 153.77, 141.85, 141.49, 141.02 (d, $J = 5.0$ Hz), 133.38, 132.43, 131.98, 129.21, 127.87, 127.25, 126.29, 118.69, 111.71, 111.07 (d, $J = 5.0$ Hz), 104.16, 103.90, 61.94, 54.63, 44.11. HRMS (ESI): exact mass calcd for $C_{23}H_{18}ClFN_5O_2^+$ $[M + H]^+$, 450.1133; found, 450.1121. HPLC purity 95.9% ($t_R = 14.27$ min).

4-((4-(5-Chloro-6-((2,3-dihydroxypropyl)amino)-2-fluoropyridin-3-yl)-1-oxophthalazin-2(1H)-yl)methyl)benzoxonitrile (19f). White solid (81% yield); mp 108.7–109.3 °C; 1H NMR (400 MHz, chloroform-*d*) δ 8.54–8.48 (m, 1H), 7.87–7.79 (m, 2H), 7.72–7.68 (m, 1H), 7.65 (d, $J = 8.0$ Hz, 2H), 7.59 (d, $J = 8.0$ Hz, 2H), 7.57–7.53 (m, 1H), 5.78 (t, $J = 6.1$ Hz, 1H), 5.49 (s, 2H), 4.00 (s, 1H), 3.82–3.74 (m, 2H), 3.72–3.60 (m, 2H), 2.87 (s, 1H), 2.59 (s, 1H). ^{13}C NMR (126 MHz, chloroform-*d*) δ 159.44, 159.10, 157.53, 154.02, 153.88, 141.83, 141.28, 141.24, 133.44, 132.45, 132.05, 129.20, 127.86, 127.29, 126.23, 118.68, 111.72, 111.16, 104.36, 104.11, 70.97, 64.01, 54.66, 44.19. HRMS (ESI): exact mass calcd for $C_{24}H_{19}ClFN_5NaO_3^+$ $[M + H]^+$, 502.1058; found, 502.1053. HPLC purity 99.0% ($t_R = 13.47$ min).

(S)-4-((4-(5-Chloro-6-((2,3-dihydroxypropyl)amino)-2-fluoropyridin-3-yl)-1-oxophthalazin-2(1H)-yl)methyl)benzoxonitrile (19g). White solid (83% yield); $[\alpha]_D^{20} -10.03$ (0.108 mg/mL, MeOH); mp 98.8–99.2 °C; 1H NMR (400 MHz, chloroform-*d*) δ 8.54–8.47 (m, 1H), 7.86–7.79 (m, 2H), 7.71–7.68 (m, 1H), 7.64 (d, $J = 8.0$ Hz, 2H), 7.58 (d, $J = 8.0$ Hz, 2H), 7.57–7.54 (m, 1H), 5.81 (t, $J = 6.1$ Hz, 1H), 5.49 (s, 2H), 4.05–3.96 (m, 1H), 3.84–3.74 (m, 2H), 3.72–3.59. HRMS (ESI): exact mass calcd for $C_{24}H_{20}ClFN_5O_3^+$ $[M + H]^+$, 480.1239; found, 480.1231. HPLC purity 98.9% ($t_R = 14.06$ min).

(R)-4-((4-(5-Chloro-6-((2,3-dihydroxypropyl)amino)-2-fluoropyridin-3-yl)-1-oxophthalazin-2(1H)-yl)methyl)benzoxonitrile (19h). White solid (79% yield); $[\alpha]_D^{20} 11.11$ (0.102 mg/mL, MeOH); mp 120.4–120.9 °C; 1H NMR (400 MHz, chloroform-*d*) δ 8.53–8.47 (m, 1H), 7.85–7.79 (m, 2H), 7.71–7.68 (m, 1H), 7.64 (d, $J = 8.0$ Hz, 2H), 7.58 (d, $J = 8.0$ Hz, 2H), 7.57–7.54 (m, 1H), 5.78 (t, $J = 6.0$ Hz, 1H), 5.49 (s, 2H), 4.00 (brs, 1H), 3.84–3.73 (m, 2H), 3.70–3.60 (m, 2H), 3.16 (s, 1H), 2.86 (s, 1H). ^{13}C NMR (126 MHz, chloroform-*d*) δ 159.44, 159.09, 157.53, 154.02, 153.88, 141.83,

141.29, 141.25, 133.44, 132.45, 132.04, 129.20, 127.87, 127.29, 126.22, 118.68, 111.73, 111.18 (d, $J = 4.8$ Hz), 104.39, 104.14, 70.98, 64.00, 54.66, 44.19. HRMS (ESI): exact mass calcd for $C_{24}H_{19}ClFN_5NaO_3^+$ $[M + H]^+$, 502.1058; found, 502.1054. HPLC purity 98.7% ($t_R = 13.46$ min).

Pharmacokinetic (PK) Analysis. All animal studies were performed according to the protocols and guidelines of the institutional care and use committee. All the procedures related to animal handling, care, and treatment in this article were performed in compliance with Agreement of the Ethics Committee on Laboratory Animal Care and the Guidelines for the Care and Use of Laboratory Animals in Shanghai, China. In PK study, 6 male ICR mice (body weight, 18–22g) were assigned randomly into two groups. One group received the test compound orally (po), and the other group was administered intravenous (iv). Test compound was dissolved in Solutol solution (DMSO/Solutol/EtOH/saline, 5/10/10/75, v/v/v/v) for iv dose and in 0.5% CMC-Na for po dose. Test compound was administered at 20 mg/kg and 2 mg/kg for po and iv route, respectively. Blood samples (20 μ L) were collected from the femoral vein at 0.25, 0.5, 1, 2, 4, 8, and 24 h into heparin-containing microcentrifuge tubes, and plasma samples were then isolated by centrifugation, followed by collection of 10 μ L of plasma and precipitation of protein immediately with ACN/MeOH (1:1, v/v) for analysis. Plasma concentrations of the test compound were analyzed using LC–MS/MS. Individual plasma concentration–time profiles were subjected to a noncompartmental pharmacokinetic analysis (NCA) using WinNonlin Professional, version 5.2.1.

In tissue distribution study, 12 male ICR mice (body weight, 18–22g) were randomly assigned into four groups corresponding to the four collection time points (1, 3, 8, and 24 h postdose), and each was orally administered with 20 mg/kg of test compound. After isoflurane inhalation anesthesia, blood samples were collected from heart and liver portal vein, respectively, and centrifuged to obtain plasma samples. After portal vein catheterization and perfusion, livers were removed from mice at designated time points. These tissues were washed with saline and dried with filter paper. For extraction, mice livers were accurately weighed and then homogenized in saline (5 mL/g tissue).

The analysis were performed on an Acquity Ultra liquid chromatography (UPLC) system (Waters Corporation, Milford, MA, USA) coupled to a Xevo TQ-S mass spectrometer (Waters Corporation, Milford, MA, USA). Chromatographic separation was performed using an Acquity UPLC BEH C18 (1.7 μ m, 2.1 mm \times 50 mm) column supplied by Waters at a flow of 0.5 mL/min. The Xevo TQ-S mass spectrometer was equipped with an electrospray ionization probe and was operated in the positive ion mode.

Microsomal Stability Assay and Metabolic Identification in Liver Microsomes. Each incubated mixture contained 0.5 mg/mL liver microsome (human, monkey, dog, rat, or mouse), 3.0 μ M test compound, and 100 mM potassium phosphate buffer (pH 7.4) in a total volume of 100 μ L. After prewarming at 37 °C for 3 min, 1 mM NADPH was added to initiate the reaction. The reaction was terminated after 60 min by adding 100 μ L of ice-cold acetonitrile into the incubation mixture. The sample was then centrifuged at 14 000 rpm for 5 min. The supernatant was then analyzed by UPLC–UV/Q-TOF MS.

HBV DNA Quantification and Cytotoxicity Assay.^{24,27} HepG2.2.15 cells (GenBank accession number U95551) were maintained in minimum essential media (MEM Gibco) supplemented with 10% fetal bovine serum (FBS Hyclone) and 380 μ g/mL G418 (Gibco). HepG2.2.15 cells were cultured and treated with different concentrations of agents in 96-well plates at a density of 4×10^3 cells for 8 days under standard conditions. HBV DNA from cell culture medium was extracted by QIA-symphony SP (Qiagen) and quantified by real-time PCR and as described previously. After the medium was collected, 100 μ L of MTT (final concentration 2.5 mg/mL, Sigma-Aldrich) was added for 1 h at 37 °C. The cells were then lysed with 10% sodium dodecyl sulfate (SDS) and 50% *N,N*-dimethylformamide, pH 7.2. OD values were read at 570 nm, and the percentage of cell death was calculated.

Southern Blotting Analysis. HepG2.2.15 cells were cultured in 12-well plates, and the HBV DNAs from the intracellular HBV capsids were extracted and detected by Southern blotting using a DIG-labeled PCR fragment according to the protocol described previously.²⁸

In Vivo Efficacy in the AAV/HBV-Infected BALB/c Mice Model. Balb/c male mice (6–8 weeks) were obtained from Shanghai Lingchang Biotechnology Co, Ltd. and kept under specific pathogen-free (SPF) conditions. Mice were injected intravenously (iv) with a recombinant adeno-associated virus (AAV) carrying the HBV 1.1 genome (10^{11} viral genome equivalents) in order to establish an alternative model of chronic HBV infection. Five weeks after injection, mice with stable viremia were selected and treated with antiviral agents for 4 weeks.²⁹ Every week, blood was collected and the levels of HBV DNA in plasma were determined by real-time PCR.

■ ASSOCIATED CONTENT

SI Supporting Information

The Supporting Information is available free of charge at <https://pubs.acs.org/doi/10.1021/acs.jmedchem.0c00346>.

Tissue distributions profiles and plasma concentration–time curves in mice of **4r**, **10m**, and **19f**; detailed experimental procedures for the synthesis of analogues **10a**, **10b**, **10i**, **10j**, **10k** and intermediates **18h**–**18n**; characterization (¹H NMR spectra and ¹³C NMR spectra are attached) and HPLC purity control of the selected final compounds **10l**, **10m**, **18a**, **18b**, **18d**, **18e**, **18g**, **19a**–**19h** (PDF)

Molecular-formula strings of the reported compounds and some data (CSV)

■ AUTHOR INFORMATION

Corresponding Authors

Li Yang – Laboratory of Immunopharmacology, Shanghai Institute of Materia Medica, Chinese Academy of Sciences, Shanghai 201203, China; Email: yangli@simm.ac.cn; Fax: +86-2150806701

Jianping Zuo – Laboratory of Immunopharmacology, Shanghai Institute of Materia Medica, Chinese Academy of Sciences, Shanghai 201203, China; Laboratory of Immunology and Virology, Shanghai University of Traditional Chinese Medicine, Shanghai 201203, China; Email: jpzuo@simm.ac.cn; Fax: +86-2150806701

Youhong Hu – State Key Laboratory of Drug Research, Shanghai Institute of Materia Medica, Chinese Academy of Sciences, Shanghai 201203, China; University of Chinese Academy of Sciences, Beijing 100049, China; School of Pharmaceutical Science and Technology, Hangzhou Institute for Advanced Study, Hangzhou 310024, China; orcid.org/0000-0003-1770-6272; Email: yhhu@simm.ac.cn; Fax: +86-2150805896

Authors

Wuhong Chen – State Key Laboratory of Drug Research, Shanghai Institute of Materia Medica, Chinese Academy of Sciences, Shanghai 201203, China

Feifei Liu – Laboratory of Immunopharmacology, Shanghai Institute of Materia Medica, Chinese Academy of Sciences, Shanghai 201203, China; University of Chinese Academy of Sciences, Beijing 100049, China

Qiliang Zhao – State Key Laboratory of Drug Research, Shanghai Institute of Materia Medica, Chinese Academy of Sciences, Shanghai 201203, China; University of Chinese Academy of Sciences, Beijing 100049, China

Xinna Ma – Laboratory of Immunopharmacology, Shanghai Institute of Materia Medica, Chinese Academy of Sciences, Shanghai 201203, China; Laboratory of Immunology and Virology, Shanghai University of Traditional Chinese Medicine, Shanghai 201203, China

Dong Lu – State Key Laboratory of Drug Research, Shanghai Institute of Materia Medica, Chinese Academy of Sciences, Shanghai 201203, China

Heng Li – Laboratory of Immunopharmacology, Shanghai Institute of Materia Medica, Chinese Academy of Sciences, Shanghai 201203, China; University of Chinese Academy of Sciences, Beijing 100049, China

Yanping Zeng – State Key Laboratory of Drug Research, Shanghai Institute of Materia Medica, Chinese Academy of Sciences, Shanghai 201203, China; University of Chinese Academy of Sciences, Beijing 100049, China

Xiankun Tong – Laboratory of Immunopharmacology, Shanghai Institute of Materia Medica, Chinese Academy of Sciences, Shanghai 201203, China

Limin Zeng – State Key Laboratory of Drug Research, Shanghai Institute of Materia Medica, Chinese Academy of Sciences, Shanghai 201203, China

Jia Liu – State Key Laboratory of Drug Research, Shanghai Institute of Materia Medica, Chinese Academy of Sciences, Shanghai 201203, China

Complete contact information is available at: <https://pubs.acs.org/doi/10.1021/acs.jmedchem.0c00346>

Author Contributions

#W.C., F.L., and Q.Z. contributed equally to this work.

Notes

The authors declare no competing financial interest.

■ ACKNOWLEDGMENTS

This project was supported by the National Natural Science Foundation of China (Grant 81872725), Science and Technology Commission of Shanghai Municipality (Grant 18431907100), the National Science Foundation of Shanghai (Grant 17ZR1436400), and National Science and Technology Major Project (Grant 2018ZX09711002-014-004).

■ ABBREVIATIONS USED

HBV, hepatitis B virus; ETV, entecavir; IFN, interferon; pgRNA, pregenomic RNA; NA, not active; SDPK, single dose pharmacokinetics; HLM, human liver microsome; SAR, structure–activity relationship; rcDNA, relaxed circular DNA; ssDNA, single-stranded DNA; PCR, polymerase chain reaction; CMC-Na, sodium carboxymethyl cellulose; b.i.d., twice daily; Cs₂CO₃, cesium carbonate; DMF, *N,N*-dimethylformamide; X-Phos, dicyclohexyl(2',4',6'-triisopropyl-[1,1'-biphenyl]-2-yl)phosphane; K₂CO₃, potassium carbonate; THF, tetrahydrofuran; DIBAL-H, diisobutylaluminum hydride; DMSO, dimethyl sulfoxide; NCS, *N*-chlorosuccinimide; NADPH, nicotinamide adenine dinucleotide phosphate

■ REFERENCES

- (1) World Health Organization Hepatitis B fact sheet. <https://www.who.int/news-room/fact-sheets/detail/hepatitis-B> (accessed July 18, 2019).
- (2) Schweitzer, A.; Horn, J.; Mikolajczyk, R. T.; Krause, G.; Ott, J. J. Estimations of worldwide prevalence of chronic hepatitis B virus infection: a systematic review of data published between 1965 and 2013. *Lancet* **2015**, *386*, 1546–1555.

- (3) EASL clinical practice guidelines: Management of chronic hepatitis B virus infection. *J. Hepatol.* **2012**, *57* (1), 167–185.
- (4) Pei, Y.; Wang, C.; Yan, S. F.; Liu, G. Past, current, and future developments of therapeutic agents for treatment of chronic hepatitis B virus infection. *J. Med. Chem.* **2017**, *60* (15), 6461–6479.
- (5) Lee, H. M.; Banini, B. A. Updates on chronic HBV: current challenges and future goals. *Curr. Treat. Options. Gastro.* **2019**, *17* (2), 271–291.
- (6) Sun, D.; Zhu, L.; Yao, D.; Chen, L.; Fu, L.; Ouyang, L. Recent progress in potential anti-hepatitis B virus agents: Structural and pharmacological perspectives. *Eur. J. Med. Chem.* **2018**, *147*, 205–217.
- (7) Zlotnick, A.; Venkatakrishnan, B.; Tan, Z.; Lewellyn, E.; Turner, W.; Francis, S. Core protein: A pleiotropic keystone in the HBV lifecycle. *Antiviral Res.* **2015**, *121*, 82–93.
- (8) Nijampatnam, B.; Liotta, D. C. Recent advances in the development of HBV capsid assembly modulators. *Curr. Opin. Chem. Biol.* **2019**, *50*, 73–79.
- (9) Yang, L.; Liu, F.; Tong, X.; Hoffmann, D.; Zuo, J.; Lu, M. Treatment of chronic hepatitis B virus infection using small molecule modulators of nucleocapsid assembly: recent advances and perspectives. *ACS Infect. Dis.* **2019**, *5* (5), 713–724.
- (10) Stray, S. J.; Zlotnick, A. BAY 41-4109 has multiple effects on hepatitis B virus capsid assembly. *J. Mol. Recognit.* **2006**, *19* (6), 542–548.
- (11) Qiu, Z.; Lin, X.; Zhou, M.; Liu, Y.; Zhu, W.; Chen, W.; Zhang, W.; Guo, L.; Liu, H.; Wu, G.; Huang, M.; Jiang, M.; Xu, Z.; Zhou, Z.; Qin, N.; Ren, S.; Qiu, H.; Zhong, S.; Zhang, Y.; Zhang, Y.; Wu, X.; Shi, L.; Shen, F.; Mao, Y.; Zhou, X.; Yang, W.; Wu, J. Z.; Yang, G.; Mayweg, A. V.; Shen, H. C.; Tang, G. Design and synthesis of orally bioavailable 4-methyl heteroaryldihydropyrimidine based hepatitis B virus (HBV) capsid inhibitors. *J. Med. Chem.* **2016**, *59* (16), 7651–7666.
- (12) Boucle, S.; Lu, X.; Bassit, L.; Ozturk, T.; Russell, O. O.; Amblard, F.; Coats, S. J.; Schinazi, R. F. Synthesis and antiviral evaluation of novel heteroarylpyrimidines analogs as HBV capsid effectors. *Bioorg. Med. Chem. Lett.* **2017**, *27* (4), 904–910.
- (13) Li, X.; Zhou, K.; He, H.; Zhou, Q.; Sun, Y.; Hou, L.; Shen, L.; Wang, X.; Zhou, Y.; Gong, Z.; He, S.; Jin, H.; Gu, Z.; Zhao, S.; Zhang, L.; Sun, C.; Zheng, S.; Cheng, Z.; Zhu, Y.; Zhang, M.; Li, J.; Chen, S. Design, synthesis, and evaluation of tetrahydropyrido[1,2-c]-pyrimidines as capsid assembly inhibitors for HBV treatment. *ACS Med. Chem. Lett.* **2017**, *8* (9), 969–974.
- (14) Qiu, Z.; Lin, X.; Zhang, W.; Zhou, M.; Guo, L.; Kocer, B.; Wu, G.; Zhang, Z.; Liu, H.; Shi, H.; Kou, B.; Hu, T.; Hu, Y.; Huang, M.; Yan, S. F.; Xu, Z.; Zhou, Z.; Qin, N.; Wang, Y. F.; Ren, S.; Qiu, H.; Zhang, Y.; Zhang, Y.; Wu, X.; Sun, K.; Zhong, S.; Xie, J.; Ottaviani, G.; Zhou, Y.; Zhu, L.; Tian, X.; Shi, L.; Shen, F.; Mao, Y.; Zhou, X.; Gao, L.; Young, J. A. T.; Wu, J. Z.; Yang, G.; Mayweg, A. V.; Shen, H. C.; Tang, G.; Zhu, W. Discovery and pre-clinical characterization of third-generation 4-H heteroaryldihydropyrimidine (HAP) analogues as hepatitis B virus (HBV) capsid inhibitors. *J. Med. Chem.* **2017**, *60* (8), 3352–3371.
- (15) Ren, Q.; Liu, X.; Yan, G.; Nie, B.; Zou, Z.; Li, J.; Chen, Y.; Wei, Y.; Huang, J.; Luo, Z.; Gu, B.; Goldmann, S.; Zhang, J.; Zhang, Y. 3-((R)-4-(((R)-6-(2-Bromo-4-fluorophenyl)-5-(ethoxycarbonyl)-2-(thiazol-2-yl)-3,6-dihydropyrimidin-4-yl)methyl)morpholin-2-yl)propanoic acid (HEC72702), a novel hepatitis B virus capsid inhibitor based on clinical candidate GLS4. *J. Med. Chem.* **2018**, *61* (3), 1355–1374.
- (16) Qiu, J.; Gong, Q.; Gao, J.; Chen, W.; Zhang, Y.; Gu, X.; Tang, D. Design, synthesis and evaluation of novel phenyl propionamide derivatives as non-nucleoside hepatitis B virus inhibitors. *Eur. J. Med. Chem.* **2018**, *144*, 424–434.
- (17) Kondylis, P.; Schlicksup, C. J.; Katen, S. P.; Lee, L. S.; Zlotnick, A.; Jacobson, S. C. Evolution of intermediates during capsid assembly of hepatitis B virus with phenylpropionamide-based antivirals. *ACS Infect. Dis.* **2019**, *5* (5), 769–777.
- (18) Sari, O.; Boucle, S.; Cox, B. D.; Ozturk, T.; Russell, O. O.; Bassit, L.; Amblard, F.; Schinazi, R. F. Synthesis of sulfamoylbenzamide derivatives as HBV capsid assembly effector. *Eur. J. Med. Chem.* **2017**, *138*, 407–421.
- (19) Vandyck, K.; Rombouts, G.; Stoops, B.; Tahri, A.; Vos, A.; Verschuere, W.; Wu, Y.; Yang, J.; Hou, F.; Huang, B.; Vergauwen, K.; Dehertogh, P.; Berke, J. M.; Raboisson, P. Synthesis and evaluation of N-phenyl-3-sulfamoyl-benzamide derivatives as capsid assembly modulators inhibiting hepatitis B virus (HBV). *J. Med. Chem.* **2018**, *61* (14), 6247–6260.
- (20) Lam, A. M.; Espiritu, C.; Vogel, R.; Ren, S.; Lau, V.; Kelly, M.; Kuduk, S. D.; Hartman, G. D.; Flores, O. A.; Klumpp, K. Preclinical characterization of NVR 3-778, a first-in-class capsid assembly modulator against hepatitis B virus. *Antimicrob. Agents Chemother.* **2019**, *63* (1), No. e01734-18.
- (21) Yuen, M. F.; Gan, E. J.; Kim, D. J.; Weilert, F.; Yuen Chan, H. L.; Lalezari, J.; Hwang, S. G.; Nguyen, T.; Flores, O.; Hartman, G.; Liaw, S.; Lenz, O.; Kakuda, T. N.; Talloen, W.; Schwabe, C.; Klumpp, K.; Brown, N. Antiviral activity, safety, and pharmacokinetics of capsid assembly modulator NVR 3-778 in patients with chronic HBV infection. *Gastroenterology* **2019**, *156* (5), 1392–1403.
- (22) Trépo, C.; Chan, H. L. Y.; Lok, A. Hepatitis B virus infection. *Lancet* **2014**, *384*, 2053–2063.
- (23) Zhou, Z.; Hu, T.; Zhou, X.; Wildum, S.; Garcia-Alcalde, F.; Xu, Z.; Wu, D.; Mao, Y.; Tian, X.; Zhou, Y.; Shen, F.; Zhang, Z.; Tang, G.; Najera, I.; Yang, G.; Shen, H. C.; Young, J. A.; Qin, N. Heteroaryldihydropyrimidine (HAP) and sulfamoylbenzamide (SBA) inhibit hepatitis B virus replication by different molecular mechanisms. *Sci. Rep.* **2017**, *7*, 42374.
- (24) Lu, D.; Liu, F.; Xing, W.; Tong, X.; Wang, L.; Wang, Y.; Zeng, L.; Feng, C.; Yang, L.; Zuo, J.; Hu, Y. Optimization and synthesis of pyridazinone derivatives as novel inhibitors of hepatitis B virus by inducing genome-free capsid formation. *ACS Infect. Dis.* **2017**, *3* (3), 199–205.
- (25) Delaney IV, W. E.; Edwards, R.; Colledge, D.; Shaw, T.; Furman, P.; Painter, G.; Locarnini, S. Phenylpropionamide derivatives AT-61 and AT-130 inhibit replication of wild-type and lamivudine-resistant strains of hepatitis B virus in vitro. *Antimicrob. Agents Chemother.* **2002**, *46* (9), 3057–3060.
- (26) Brezillon, N.; Brunelle, M. N.; Massinet, H.; Giang, E.; Lamant, C.; DaSilva, L.; Berissi, S.; Belghiti, J.; Hannoun, L.; Puerstinger, G.; Wimmer, E.; Neyts, J.; Hantz, O.; Soussan, P.; Morosan, S.; Kremsdorf, D. Antiviral activity of Bay 41-4109 on hepatitis B virus in humanized Alb-uPA/SCID mice. *PLoS One* **2011**, *6* (12), No. e25096.
- (27) Wang, Y.; Lu, D.; Xu, Y.; Xing, W.; Tong, X.; Wang, G.; Feng, C.; He, P.; Yang, L.; Tang, W.; Hu, Y.; Zuo, J. A novel pyridazinone derivative inhibits hepatitis B virus replication by inducing genome-free capsid formation. *Antimicrob. Agents Chemother.* **2015**, *59* (1), 7061–7072.
- (28) Yang, L.; Shi, L.; Chen, H.; Tong, X.; Wang, G.; Zhang, Y.; Wang, W.; Feng, C.; He, P.; Zhu, F.; Hao, Y.; Wang, B.; Yang, D.; Tang, W.; Nan, F.; Zuo, J. Isothiafludine, a novel non-nucleoside compound, inhibits hepatitis B virus replication through blocking pregenomic RNA encapsidation. *Acta Pharmacol. Sin.* **2014**, *35*, 410–418.
- (29) Di Scala, M.; Otano, I.; Gil-Farina, I.; Vanrell, L.; Hommel, M.; Olagüe, C.; Vales, A.; Galarraga, M.; Guembe, L.; Ortiz de Solorzano, C.; Ghosh, I.; Maini, M. K.; Prieto, J.; González-Aseguinolaza, G. Complementary effects of interleukin-15 and alpha interferon induce immunity in hepatitis B virus transgenic mice. *J. Virol.* **2016**, *90* (19), 8563–8574.